



Soodmand, S., Morris, K. A., & Beach, M. A. (2021). *Quantization of Impedance Stability in Frequency Domain*. Paper presented at 2021 International Electrical Engineering Congress (iEECON 2021), Pattaya, Thailand.

Peer reviewed version

[Link to publication record in Explore Bristol Research](#)  
PDF-document

## University of Bristol - Explore Bristol Research

### General rights

This document is made available in accordance with publisher policies. Please cite only the published version using the reference above. Full terms of use are available:  
<http://www.bristol.ac.uk/red/research-policy/pure/user-guides/ebr-terms/>

# Quantization of Impedance Stability in Frequency Domain

Soheyl Soodmand  
dept.electrical & electronic engineering  
university of bristol  
Bristol, United Kingdom  
soheyl.soodmand2@gmail.com

Kevin A. Morris  
dept.electrical & electronic engineering  
university of bristol  
Bristol, United Kingdom  
kevin.morris@bristol.ac.uk

Mark A. Beach  
dept.electrical & electronic engineering  
university of bristol  
Bristol, United Kingdom  
m.a.beach@bristol.ac.uk

**Abstract**—A method based on Sample Standard Deviation (SSD) is suggested here to quantify impedance stability in frequency domain. Firstly, impedance instability factor,  $\delta_T$ , is introduced as an indicator of that could be used for impedance stability quantifications of measured or simulated impedance data of Radio Frequency (RF) and high-power devices. The method is used then for a generic real/imaginary impedance trajectory as an example to clarify calculation process. Finally, the introduced approach has been used to quantify impedance stabilities in some RF devices such as stable impedance antenna of 5G In-Band Full Duplex (IBFD) Transceivers, microstrip low-pass filter and hybrid coupler. Also, suitable efficiency of the method to follow up correct design direction to smoothen impedance of an antenna is realized.

**Keywords**— microwave measurement, impedance stability, RF devices, high power, antennas, IBFD.

## I. INTRODUCTION

Acquisition of impedance stability in frequency domain is an important feature to retain suitable efficiency in systems such as: 5G In-Band Full Duplex Transceivers (IBFD) [1]–[3], biotelemetric devices [4], [5], body-Centric antennas [6], [7], ultra-wideband (UWB) systems [8], impedance-matching tuners [9], nanoantenna for THz communication [10], power amplifiers [11], mechatronic systems [12], microwires [13], power inverters/generators [14], grid distribution networks [15], and high frequency oscillation eliminators in medium-voltage direct-current (MVDC) systems [16]. Examples of some of these systems are shown in Fig. 1. To the best of the authors knowledge there is not any specific mathematical method in the literature to quantify impedance stability in frequency domain and normally visual methods are carried out for these assessments. Quantifying impedance stability could help designers to follow up efficient design direction when a stable impedance is needed.

In this paper, Section II, a method based on Sample Standard Deviation (SSD) is suggested to quantify impedance stability in frequency domain. SSD is used as an indicator by introducing impedance instability factor,  $\delta_T$ , of that could be used for impedance stability quantifications of measured or simulated impedance data of Radio Frequency (RF) and high-power devices. The method is used then in Section III for a generic form of impedance as an example to clarify  $\delta_T$  calculation process. In Section IV, the introduced approach has been used to quantify impedance stabilities in some RF devices. Finally, a conclusion is given in Section V.

## II. SAMPLE STANDARD DEVIATION AND IMPEDANCE INSTABILITY FACTOR

Sample Standard Deviation ( $\delta$ ) in mathematics is a quantity expressing by how much the members of a data group differ from the data mean value,  $M$ , for the group. There are formulas to calculate  $\delta$  value for both continuous data function [17] and discrete data group [18]. Normally impedance trajectories of RF devices do not follow a known mathematical function in the real world, so the discrete data formula is considered here to start which is expressed [18] as

$$\delta = \sqrt{\frac{1}{N-1} \sum_{i=1}^N (x_i - M)^2} . \quad (1)$$

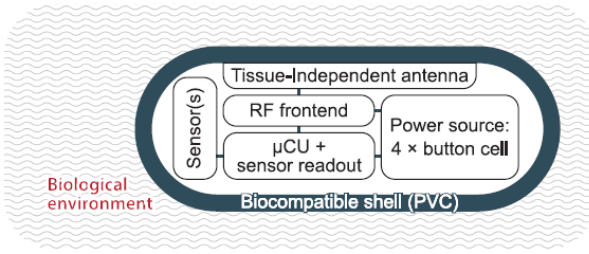
where  $\{x_1, x_2, \dots, x_N\}$  are the observed data values of the sample items,  $N$  is the number of observations in the sample and  $M = (x_1 + x_2 + \dots + x_N)/N$  is the mean value of the observed data group. Accuracy of  $\delta$  calculation increases when  $N$  increases. The  $\delta$  value is used here as an indicator to quantify impedance instability in frequency domain. The  $\delta$  parameter in (1) is rewritten for real (Re) and imaginary (Im) impedances of the device (high power, RF, or antenna), in a defined frequency bandwidth, respectively, as below

$$\delta_{Re} = \sqrt{\frac{1}{N_f-1} \sum_{i=1}^{N_f} (Z_{i(Re)} - M_{Re})^2} . \quad (2)$$

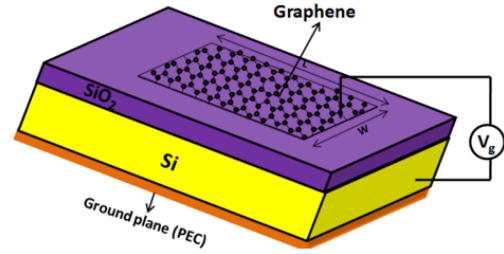
$$\delta_{Im} = \sqrt{\frac{1}{N_f-1} \sum_{i=1}^{N_f} (Z_{i(Im)} - M_{Im})^2} . \quad (3)$$

$N_f$  indicates the number of frequencies wherein either real or imaginary impedance are sampled (observed),  $Z_{i(Re)}$  and  $Z_{i(Im)}$  indicate the value of observed real and imaginary impedances respectively at each  $f_i$  frequency ( $i=1, 2, \dots, N$ ).  $M_{Re}$  and  $M_{Im}$  are mean values of sampled real and imaginary impedances, respectively.  $\delta_{Re}$  and  $\delta_{Im}$  indicates how much their relevant impedance trajectory differ from its mean value in a defined frequency bandwidth. Looking to the formulas from dimensional point of view both  $\delta_{Re}$  and  $\delta_{Im}$  have Ohm ( $\Omega$ ) unit. However, total value of  $\delta$ , so called impedance instability factor of  $\delta_T$ , is defined as a Root Mean Square (RMS) of  $\delta_{Re}$  and  $\delta_{Im}$  to quantify instability of the whole complex impedance as

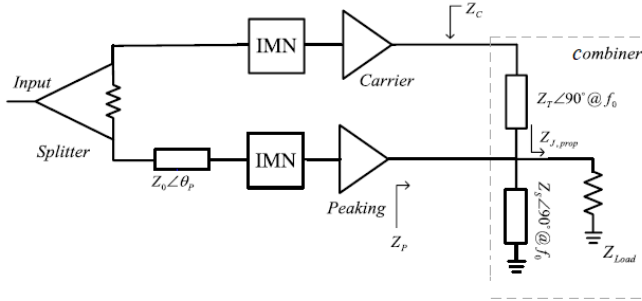
$$\delta_T = \delta_{Total} = \delta_{RMS} = \sqrt{\frac{\delta_{Re}^2 + \delta_{Im}^2}{2}} . \quad (4)$$



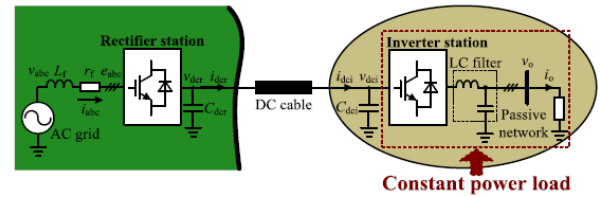
(a)



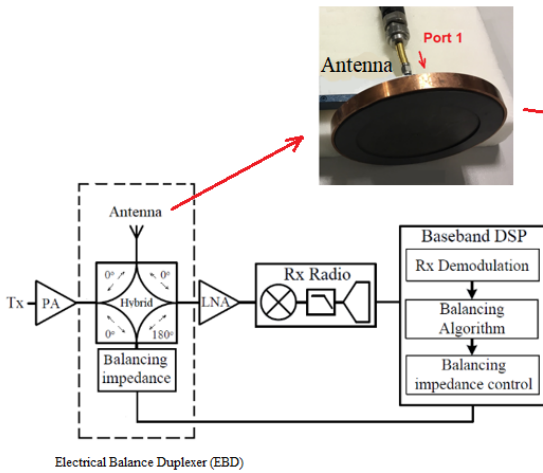
(b)



(c)



(d)



(e)

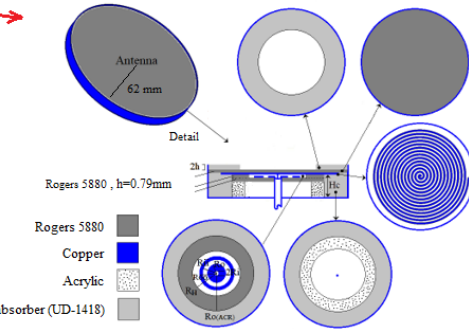


Fig. 1. Some example of systems wherein impedance stability in frequency domain is needed, (a) Wireless pill-shaped device for biotelemetry applications [5], (b) Graphene plasmonic nanoantenna for THz communication [10], (c) Doherty power amplifier with wideband combiner [11], (d) Two-terminal voltage source converter of high voltage direct current system [14], (e) In-Band Full Duplex (IBFD) RF front-end system with stable impedance antenna designed by the authors at University of Bristol.

$\delta_T$  has an ohm ( $\Omega$ ) dimension, also  $\delta_T = 0 \Omega$  indicates no impedance variations in frequency domain which is not normally possible in practice for a real RF or high-power device due to physics of electromagnetic waves. Based on the above discussion higher and lower impedance instability factors indicate lower and higher impedance stabilities, respectively and the value of  $\delta_T$  could be used as an indicator to quantify

impedance instability in frequency domain for antennas, RF and high-power devices.

### III. AN EXAMPLE TO CLARIFY $\delta_T$ CALCULATION PROCESS FOR A GENERIC FORM OF IMPEDANCE TRAJECTORY

A generic set of real and imaginary trajectories of device impedance in a defined frequency bandwidth are shown in Fig. 2 for three observation frequencies of  $f_i$  i.e. ( $i = 1, 2, 3$ ) or  $N_f = 3$ .

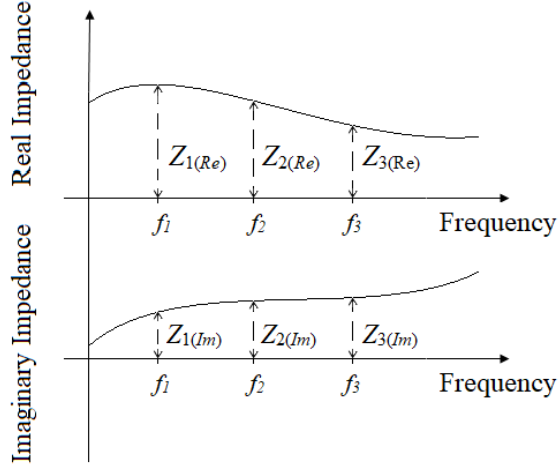


Fig. 2. Generic set of real and imaginary trajectories of antenna input impedance.

Real and imaginary impedances at frequency of  $f_i$  are denoted by  $Z_{i(Re)}$  and  $Z_{i(Im)}$ , respectively. In the first step, mean value of observed  $Z_{i(Re)}$  and  $Z_{i(Im)}$  impedances are calculated respectively as  $M_{Re} = (Z_{1(Re)} + Z_{2(Re)} + Z_{3(Re)}) / N_f$  and  $M_{Im} = (Z_{1(Im)} + Z_{2(Im)} + Z_{3(Im)}) / N_f$ , Fig. 2. Thereafter the below expressions from (2) and (3) are calculated as

$$\sum_{i=1}^3 (Z_{i(Re)} - \mu_{Re})^2 = (Z_{1(Re)} - M_{Re})^2 + (Z_{2(Re)} - M_{Re})^2 + (Z_{3(Re)} - M_{Re})^2. \quad (5)$$

$$\sum_{i=1}^3 (Z_{i(Im)} - M_{Im})^2 = (Z_{1(Im)} - M_{Im})^2 + (Z_{2(Im)} - M_{Im})^2 + (Z_{3(Im)} - M_{Im})^2. \quad (6)$$

Now the resulted values from (5) and (6) replaced respectively in (2) and (3) with  $N_f=3$  to calculate  $\delta_{Re}$  and  $\delta_{Im}$ . Finally, the calculated  $\delta_{Re}$  and  $\delta_{Im}$  values are replaced in (4) to obtain impedance instability factor of  $\delta_T$ . It needs to be mentioned that choosing  $N_f = 3$  causes a low accuracy in  $\delta_T$  calculations and in practice higher number of observation frequencies i.e. higher  $N_f$  is needed for precise calculation, for example  $N_f = 500$  is used in this paper for calculations. The described method could be used to quantify impedance instability.

#### IV. ASSESSMENTS

Firstly, impedance trajectories of some RF devices have been evaluated in this section to calculate their impedance instability factor. These are three RF devices: a stable impedance antenna for IBFD applications (Fig. 1(e)), a microstrip low pass filter (Fig. 3) and a microstrip hybrid coupler (Fig. 3). Measured impedances of these devices by Vector Network Analyzer (VNA) are shown in Fig. 4 where their calculated  $\delta_{Re}$ ,  $\delta_{Im}$  and impedance instability factor of  $\delta_T$  at 2GHz - 3.5GHz range are

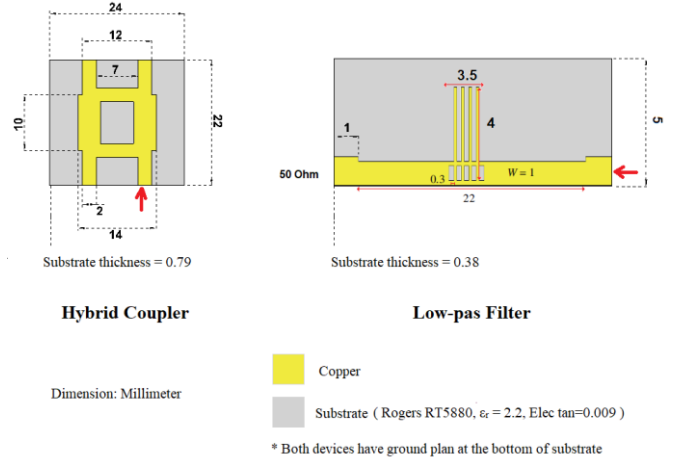


Fig. 3. Assessed hybrid coupler and low-pass filter.

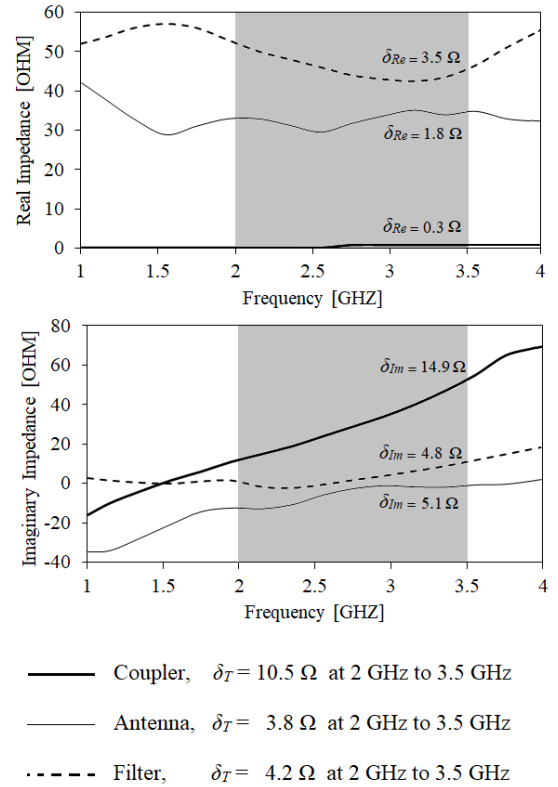


Fig. 4. Impedance and  $\delta_T$  factor of antenna (Fig. 1(e)), coupler (Fig. 3) and low pass filter (Fig. 3).

calculated as well based on the method and formulas described in Section II and Section III, indicating how much their impedance trajectory differ from its mean value in the defined frequency bandwidth. Measurements are performed at the port shown by red arrow (Fig. 1(e) and Fig.3) while for coupler and filter the other ports are terminated by 50  $\Omega$  broadband load.

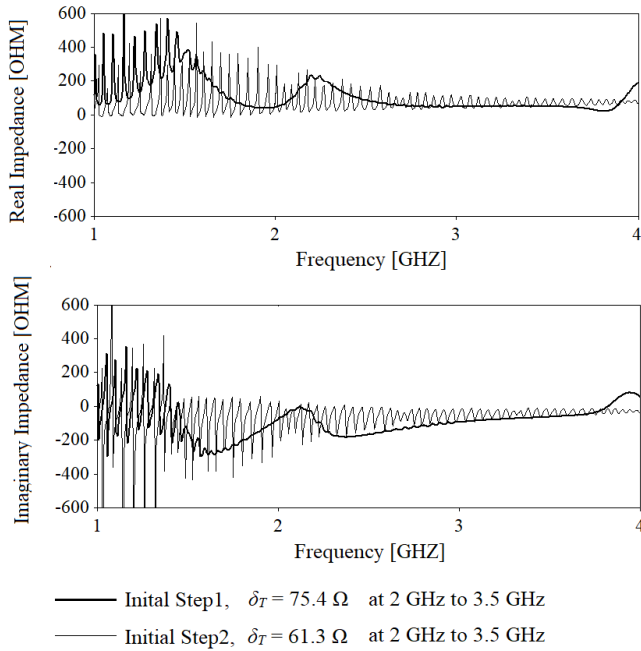


Fig. 5. Impedance and  $\delta_T$  factor of antenna at the initial steps of design.

Secondly, in the cases wherein the designer faces with very dense impedance variation in the design process, the introduced method could help to follow up more efficient design direction. An example of impedance trajectory with dense impedance variation is shown in Fig. 5 which the authors faced during initial design steps of the stable impedance antenna shown in Fig1(e). Final smoothed impedance of the antenna, with lower impedance instability indicator of  $\delta_T$ , is achieved following up the presented impedance stability quantization method (Section II and Section III) to reduce  $\delta_T$  indicator in step-by-step modifications and the result is given in Fig. 4, confirming efficiency of the introduced method to achieve stable impedance.

The design process of the stable impedance antenna is given with more details in a separate paper and the focus of this paper here was on quantization of impedance stability in frequency domain by introducing impedance instability factor,  $\delta_T$ , in theory and then assessment based on measured data of some practical devices.

## V. CONCLUSION

Sample Standard Deviation (SSD) based method is suggested in this paper to quantify impedance stability in frequency domain. Impedance instability factor,  $\delta_T$ , is introduced as an indicator of that could be used for impedance instability quantifications of measured and simulated impedance data of Radio Frequency (RF) and high-power devices. The method is used then for a generic real/imaginary impedance trajectory to clarify calculation process. The introduced method then has been used to quantify impedance instabilities in some RF devices: a stable impedance antenna for IBFD applications, a low pass filter, and a microstrip hybrid

coupler. Also, suitable efficiency of the method to follow up correct design direction to smoothen impedance of an IBFD antenna is realized.

## REFERENCES

- [1] L. Laughlin, C. Zhang, M. A. Beach, K. A. Morris, and J. L. Haine, "Passive and active electrical balance duplexers," *IEEE Trans. Circuits Syst. II Express Briefs*, vol. 63, no. 1, pp. 94–98, 2016.
- [2] L. Laughlin, C. Zhang, M. A. Beach, K. A. Morris, and J. Haine, "A widely tunable full duplex transceiver combining electrical balance isolation and active analog cancellation," in *IEEE 81st Veh. Tech. Conf.*, 2015, vol. 2015, pp. 1–5.
- [3] L. Laughlin, M. A. Beach, K. A. Morris, and J. L. Haine, "Electrical balance duplexing for small form factor realization of in-band full duplex," *IEEE Commun. Mag.*, vol. 53, no. 5, pp. 102–110, 2015.
- [4] A. Basir and H. Yoo, "A Stable Impedance-Matched Ultrawideband Antenna System Mitigating Detuning Effects for Multiple Biotelemetry Applications," *IEEE Trans. Antennas Propag.*, vol. 67, no. 5, pp. 3416–3421, 2019.
- [5] D. Nikolayev, M. Zhadobov, and R. Sauleau, "Immune-To-Detuning Wireless In-Body Platform for Versatile Biotelemetry Applications," *IEEE Trans. Biomed. Circuits Syst.*, vol. 13, no. 2, pp. 403–412, 2019.
- [6] Z. Bao, Y. X. Guo, and R. Mittra, "An Ultrawideband Conformal Capsule Antenna With Stable Impedance Matching," *IEEE Trans. Antennas Propag.*, vol. 65, no. 10, pp. 5086–5094, 2017.
- [7] A. Alomainy, A. Sani, A. Rahman, J. G. Santas, and Y. Hao, "Transient characteristics of wearable antennas and radio propagation channels for ultrawideband body-centric wireless communications," *IEEE Trans. Antennas Propag.*, vol. 57, no. 4 PART. 1, pp. 875–884, 2009.
- [8] P. G. Ingerson and P. E. Mayes, "Log-Periodic Antennas with Modulated Impedance Feeders," *IEEE Trans. Antennas Propag.*, vol. 16, no. 6, pp. 633–642, 1968.
- [9] Y. Do Chung, C. Y. Lee, W. S. Lee, and E. Y. Park, "Operating Characteristics for Different Resonance Frequency Ranges of Wireless Power Charging System in Superconducting MAGLEV Train," *IEEE Trans. Appl. Supercond.*, vol. 29, no. 5, 2019.
- [10] S. Dash, A. Patnaik, and B. K. Kaushik, "Performance enhancement of graphene plasmonic nanoantennas for THz communication," *IET Microwaves, Antennas Propag.*, vol. 13, no. 1, pp. 71–75, 2019.
- [11] S. Chen, G. Wang, Z. Cheng, and Q. Xue, "A Bandwidth Enhanced Doherty Power Amplifier with a Compact Output Combiner," *IEEE Microw. Wirel. Compon. Lett.*, vol. 26, no. 6, pp. 434–436, 2016.
- [12] H. Woo and K. Kong, "Controller design for mechanical impedance reduction," *IEEE/ASME Trans. Mechatronics*, vol. 20, no. 2, pp. 845–854, 2015.
- [13] J. S. Liu, J. F. Sun, D. W. Xing, and X. Xue, "Twin-detector sensor of Co-rich amorphous microwires to overcome GMI fluctuation induced by ambient temperature," *IEEE Trans. Magn.*, vol. 48, no. 9, pp. 2449–2454, 2012.
- [14] W. Wu *et al.*, "A virtual phase-lead impedance stability control strategy for the maritime VSC-HVDC system," *IEEE Trans. Ind. Informatics*, vol. 14, no. 12, pp. 5475–5486, 2018.
- [15] M. A. Azzouz and E. F. El-Saadany, "Multivariable DG Impedance Modeling and Reshaping for Impedance Stabilization of Active Distribution Networks," *IEEE Trans. Smart Grid*, vol. 9, no. 3, pp. 2166–2179, 2018.
- [16] L. Zhou *et al.*, "Virtual Positive-Damping Reshaped Impedance Stability Control Method for the Offshore MVDC System," *IEEE Trans. Power Electron.*, vol. 34, no. 5, pp. 4951–4966, 2019.
- [17] J. Orloff and J. Bloom, "18.05 Introduction to Probability and Statistics," Massachusetts Institute of Technology: MIT OpenCourseWare, 2014.
- [18] J. F. Kenney and E. S. Keeping, *Mathematics of Statistics, Pt. 1*, 3rd ed. Princeton, NJ: Van Nostrand, 1962.